TNF-α signaling drives myeloid skewing and clonal expansion of stem and progenitor cells in *RUNX1*-familial platelet disorder

RUNX1-familial platelet disorder (FPD) is an autosomal dominant disease caused by germline *RUNX1* loss-of-function mutations. *RUNX1*-FPD is one of the most common inherited forms of myeloid malignancies.[1] Over 250 families in the USA have been identified, and a recent estimate indicates that ~18,000 patients exist.[2] *RUNX1*-FPD patients suffer from platelet dysfunction, thrombocytopenia, and increased inflammatory diseases, and about 40-50% of the patients have a lifelong risk of developing hematologic malignancies, especially myelodysplastic syndromes and acute myeloid leukemia (AML), with a median onset age of 29 years (range, 6-76 years).[3] Currently, there is a lack of early intervention or prevention strategies to protect *RUNX1*-FPD patients from developing hematologic malignancies.

Recently, we and others identified that the *RUNX1*-FPD bone marrow microenvironment is highly inflammatory, and many inflammatory pathways, including tumor necrosis factor (TNF)-α signaling, are significantly enriched in *RUNX1*-FPD hematopoietic stem and progenitor cells (HSPC) compared to healthy controls.[4-6] However, the role of TNF-α signaling in *RUNX1*-FPD hematopoiesis and evolution has not been fully demonstrated. Previous studies have shown that TNF-α is implicated in cytotoxicity against tumor cells, immunomodulation, and inflammatory responses. TNF-α is primarily produced by immune cells, such as macrophages and T cells, and leukemia stem cells to promote cell survival and treatment resistance. TNF-α upregulation drives leukemia transformation from a pre-malignant state, as demonstrated in both *in vivo* and *in vitro* models using *Dnmt3A*$^{R882/+}$ and the Fanconi anemia mouse model.[7,8] TNF-α antagonists are approved for treating autoimmune diseases effectively, but have not yet been examined as early intervention strategies in AML. In this study, we demonstrate that TNF-α drives resistance to inflammatory stress-mediated exhaustion, characterized by an increased myeloid bias of *RUNX1*-FPD progenitors, compared to healthy controls, through transcriptomic and epigenetic mechanisms. Furthermore, inhibition of TNF-α signaling in *RUNX1*-FPD rescues the differentiation defects of progenitors in murine models and human cells.

Specifically, we utilized *RUNX1*-FPD bone marrow samples from the pre-leukemia stage, obtained from the National Institutes of Health (NCT03854318), as approved by the Institutional Review Board. Mononuclear cells and CD34$^+$ progenitors were purified. Healthy bone marrow samples were age- and gender-matched to serve as controls (*Online Supplementary Table S1*). The pathway enrichment analysis of upregulated genes from published single-cell RNA-sequencing data revealed enrichment of TNF-α signaling in *RUNX1*-FPD compared to controls (Figure 1A).[4] We validated these results using bulk RNA-sequencing on *RUNX1*-FPD and healthy CD34$^+$ progenitors (Figure 1B). Differentially expressed genes in *RUNX1*-FPD showed upregulation of inflammatory pathways, including TNF-α signaling (Figure 1C, D) and RELA transcription factor, a mediator of TNF-α signaling (Figure 1E). The expression of TNF-α receptors is significantly upregulated for TNFR2 (TNFRSF1B) but not TNFR1 (TNFRSF1A) in *RUNX1*-FPD HSPC compared to healthy controls (Figure 1F). Previous cytokine analysis[4] of bone marrow extracellular fluid from FPD subjects also showed elevated levels of TNF-α and soluble TNF-RII receptor (Figure 1G). Consistent with findings in *RUNX1*-FPD patients, TNFR2 (TNFRSF1B), but not TNFR1 (TNFRSF1A), was also upregulated in *RUNX1*-mutated AML patients' samples compared to *RUNX1*-wildtype samples (*Online Supplementary Figure S1A, B*). To identify the impact of TNF-α on *RUNX1*-FPD HSPC growth and differentiation, we performed a colony-forming assay using primary bone marrow CD34$^+$ progenitors derived from *RUNX1*-FPD and healthy individuals. We demonstrated that *RUNX1*-FPD HSPC have significantly more colony formation ability compared to healthy HSPC. Both *RUNX1*-FPD and healthy HSPC exhibited slight growth suppression upon TNF-α stimulation (Figure 1H), suggesting that TNF-α may be cytotoxic to progenitors. However, *RUNX1*-FPD HSPC maintained an increased myeloid bias (colony-forming units – granulocyte-macrophage) under TNF-α-mediated inflammatory stress. Overall, these results show that the upregulated TNF-α signaling enhanced the myeloid bias of *RUNX1*-FPD HSPC (Figure 1H).

To understand how TNF-α affects myeloid bias in *RUNX1*-FPD bone marrow cells, we performed 10X single-cell RNA-sequencing using *RUNX1*-FPD mononuclear cells (N=2) treated to TNF-α and its inhibitor, etanercept. We identified 11 cell clusters across the vehicle and treated samples (*Online Supplementary Figure S2A*). Exposure of bone marrow cells to TNF-α resulted in the expansion of the monocytic-macrophage (Mono/Mac), hematopoietic stem cell (HSC), and progenitor populations (HSC/progenitors >1.7-fold) while suppressing T cells by 2-fold (Figure 2A). However, etanercept treatment did not affect HSC/progenitors while slightly suppressing Mono/Mac populations.

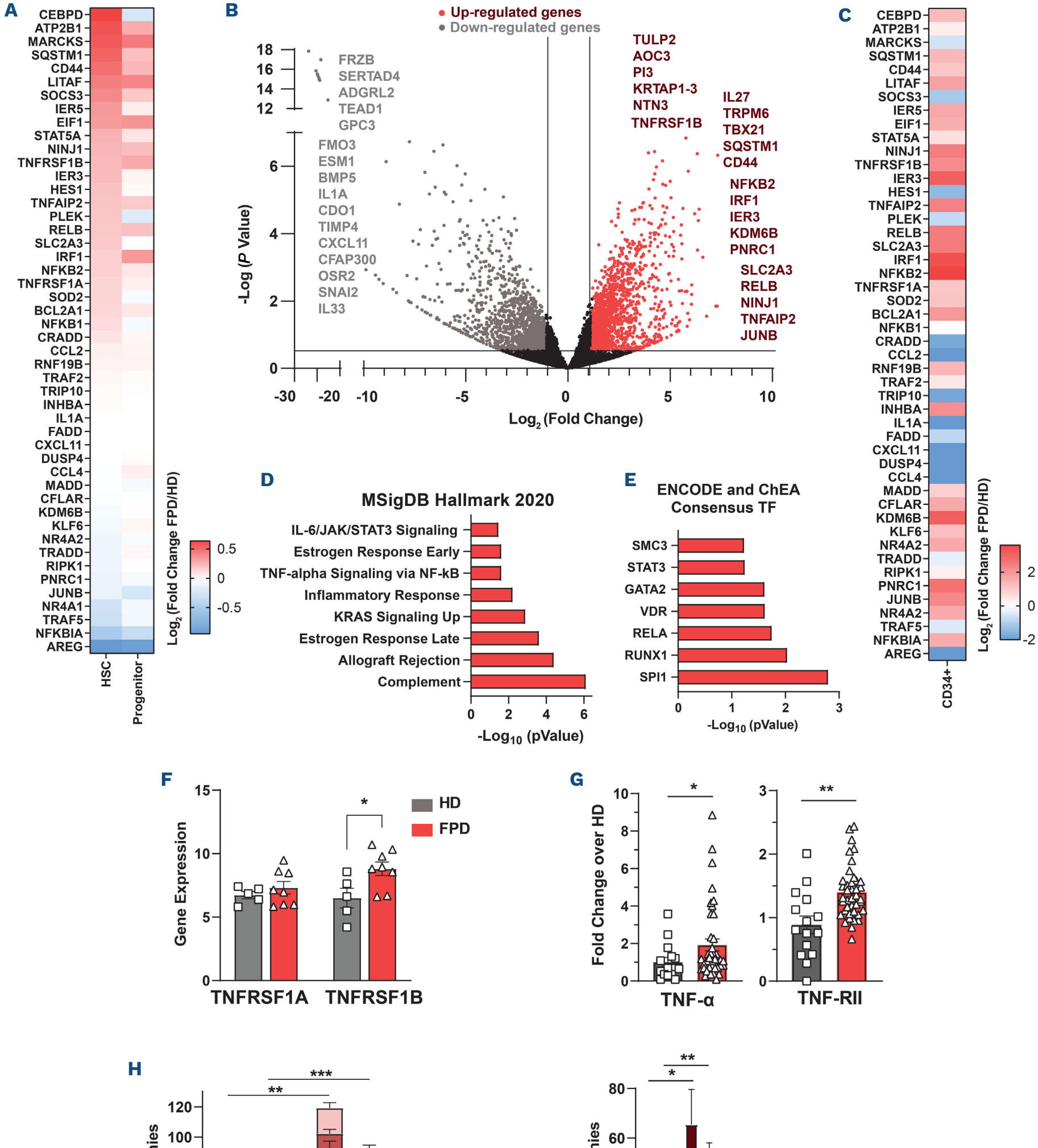

Continued on following page.

Figure 1. Tumor necrosis factor-α signaling is upregulated in *RUNX1*-familial platelet disorder compared to healthy controls. (A) Differential gene expression between patients with *RUNX1*-familial platelet disorder (FPD, N=10) and healthy controls (HD, N=4) using single-cell RNA-sequencing analysis. The genes are selected based on published databases for the leading genes in the tumor necrosis factor (TNF)-α signaling pathway. (B) The bulk RNA-sequencing analysis was performed using purified CD34⁺ cells. The volcano plot shows upregulated (red) and downregulated (gray) genes in *RUNX1*-FPD (N=8) over HD (N=5) CD34⁺ cells. (C) Expression of the leading genes in the TNF-α signaling pathway in bulk RNA-sequencing analysis. (D) Pathway analysis on significantly (*P* adjusted <0.05) upregulated (>2-fold) genes in *RUNX1*-FPD compared to HD. The analysis was done using the Enrichr database. (E) Enrichment of transcription factors in upregulated genes (*P* adjusted <0.05, >2-fold) in *RUNX1*-FPD compared to HD was assessed using the Enrichr database. (F) Expression of TNF-α receptors is shown using bulk RNA-sequencing analysis of hematopoietic stem and progenitor cells (HSPC). (G) TNF-α and TNF-RII levels in *RUNX1*-FPD (N=40) bone marrow fluid compared to those of HD (N=15), as evaluated using 65-plex luminex assay. The data are presented as fold change over average HD values. (H) The results of the colony-forming assay of *RUNX1*-FPD and HD CD34⁺ HSPC in the presence of TNF-α cytokine. Primary CD34⁺ cells were seeded at a density of 1,000 cells/well and treated with TNF-α at 1.0 ng/mL using Methocult (StemCell, H4434). Colonies were counted on day 14 after seeding. Statistical significance was calculated using the Student *t* test and differences between FPD and HD samples, or untreated and treated groups, are indicated as **P*≤0.05, ***P*≤0.01, ****P*≤0.001. CFU-M: colony-forming unit (CFU)–macrophage; CFU-G: CFU–granulocyte; CFU-GM: CFU–granulocyte/monocyte; CFU-GEMM: colony-forming unit–granulocyte, erythrocyte, megakaryocyte, monocyte; BFU-E: burst-forming unit–erythroid.

Gene set enrichment analysis of differentially expressed genes in the HSC/progenitors showed that TNF-α exposure led to the upregulation of inflammatory response pathways and TNF-α signaling, and etanercept treatment led to its suppression compared to vehicle-treated *RUNX1*-FPD cells (Figure 2B). In addition, TNF-α upregulated mTORC1 and IL-6/JAK/STAT3 pathways, and etanercept treatment inhibited these pathways, suggesting that etanercept can suppress increased inflammation and mTORC1 and JAK/STAT signaling. Recently, we demonstrated that FPD HSPC exhibit a differentiation bias towards myeloid cells and fewer megakaryocytes, resulting from the upregulation of CD74-mediated inflammation via PI3K/mTORC1 and JAK/STAT signaling.[4] Activation of the CD74 pathway was shown to induce expression and secretion of TNF-α.[9] Furthermore, TNF-α-dependent inflammation contributed to the progression of lung adenocarcinoma by upregulating MIF/CD74 in a positive feedback loop,[10] suggesting that TNF-α could also be part of the CD74 axis. Our data also suggest that increased TNF-α promotes cytotoxicity in progenitors by increasing oxidative phosphorylation, reactive oxygen species, and DNA damage pathways, leading to increased apoptosis, which we also found to be upregulated in gene set enrichment analyses. Etanercept reverses these effects, suggesting that it may improve stem cell functions by enhancing their tolerance to inflammatory stress. Overall, these results show that TNF-α signaling promotes myeloid cell expansion in *RUNX1*-FPD, and etanercept treatment rescues these effects.

Next, we evaluated how TNF-α signaling is upregulated in *RUNX1*-FPD. Our bulk RNA-sequencing analysis showed enrichment of the RELA transcription factor in *RUNX1*-FPD (Figure 1E). We, therefore, utilized a publicly available chromatin immunoprecipitation-sequencing dataset to investigate the extent of RELA binding at the transcription start site (TSS) of TNF-α and its receptors. We observed that RELA binding is enhanced in the monocytic AML cell line (THP1) at the TNF-α gene, compared to the non-monocytic cell line (K562), and RELA binding on TNF-α and TNF receptors is stronger with TNF-α treatment in the non-monocytic cell line (Figure 2C). To understand the effect of TNF-α on chromatin accessibility, we performed 10X single-cell ATAC (assay for transposase-accessible chromatin) sequencing on healthy and FPD mononuclear cells. We observed that the RELA TSS is more accessible in *RUNX1*-FPD than in healthy controls. Interestingly, RELA accessibility in the monocyte population increased with TNF-α stimulation and decreased with etanercept, indicating that high TNF-α in *RUNX1*-FPD enhances chromatin accessibility at the TSS of the RELA, which may upregulate TNF-α signaling through a positive feedback mechanism (Figure 2D).

The TNF-α signaling inhibitor etanercept is approved for treating patients with rheumatoid arthritis and psoriasis.[11] Since TNF-α is a major driver of inflammation, it could be an attractive approach in leukemia treatment and should be further evaluated.[7] To determine the impact of etanercept on the function of *RUNX1*-FPD progenitors, we first evaluated its effect on the viability of *RUNX1*-FPD bone marrow cells using an *in vitro* concentration gradient (*Online Supplementary Figure S2B*). *RUNX1*-FPD and healthy bone marrow cells maintained a viability of greater than 90% for the etanercept dose curve tested. Next, we quantified the effect of etanercept on *RUNX1*-FPD mononuclear cells on the differentiation of myeloid and megakaryocytes. We showed a significant decrease in monocyte (CD14⁺/13⁺) and an increase in megakaryocyte (CD41⁺/61⁺) cell populations (Figure 3A). Etanercept also decreased levels of CCL24, CXCL8, and M-CSF cytokines (*Online Supplementary Figure S2C*). The treatment of *RUNX1*-FPD bone marrow cells with etanercept also reduced the phosphorylation of proteins involved in PI3K/mTOR and NF-κB signaling, including p65, AKT, SRC, S6, and 4EBP1 (Figure 3B), validating the RNA-sequencing analysis (Figure 2B). Additionally, etanercept resulted in a significant reduction in colony formation ability in *RUNX1*-FPD with minimal impact on healthy controls (Figure 3C, *Online Supplementary Figure S2D*).

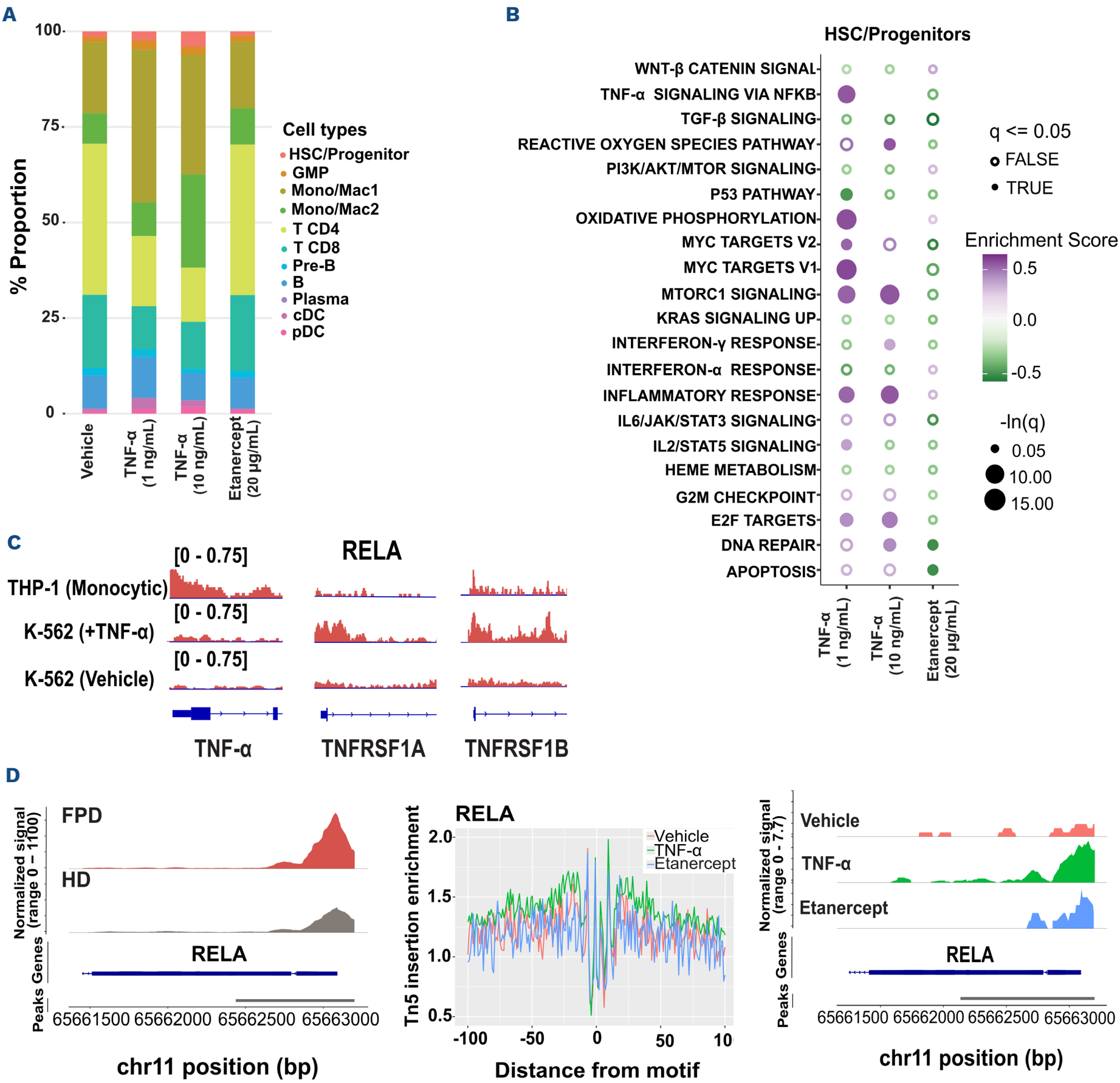

Figure 2. Single-cell transcriptomic analysis shows the expansion of myeloid cells upon tumor necrosis factor-α treatment in *RUNX1*-familial platelet disorder. (A) *RUNX1*-familial platelet disorder (FPD, N=2) bone marrow cells were treated overnight with tumor necrosis factor (TNF)-α (1 ng/mL and 10 ng/mL) and etanercept (20 µg/mL). Cells were then subjected to 10X Chromium single-cell RNA-sequencing. Approximately 2,600 cells were analyzed in the vehicle group, 2,200 cells in the TNF-α (1 ng/mL) group, 1,700 cells in the TNF-α (10 ng/mL) group, and 2,100 cells in the etanercept-treated group. The percentage of each cell population in different treatment groups is shown in bar graphs. (B) Differential expression analysis of each treatment over vehicle was performed using the FindMarkers function from Seurat and gene set enrichment analysis (GSEA) was performed using the clusterProfiler package (v4.10.1). GSEA of differentially expressed genes in each treatment group compared to vehicle-treated cells showed enrichment of different pathways. (C) RELA binding at the transcription start site (TSS) of TNF-α, TNFRSF1A, and TNFRSF1B genes in THP-1 (monocytic, SRX4001967) and K-562 (+TNF-α, SRX14499808; vehicle, SRX2424413) cell lines, plotted from public datasets using the ChIP-Atlas (*https://chip-atlas.org/*). (D) *RUNX1*-FPD bone marrow cells were treated overnight with TNF-α (1 ng/mL) and etanercept (20 µg/mL). Cells were then subjected to 10X single-cell assay for transposase-accessible chromatin (ATAC) sequencing along with healthy donor (HD) bone marrow cells. Coverage plot showing chromatin accessibility on the RELA TSS region in *RUNX1*-FPD and HD monocytes (left). Footprint profile plot (middle) of RELA in monocytes. Coverage plot (right) showing the normalized signal of open chromatin along the RELA TSS in FPD. Single-cell data are available through the dbGAP accession ID. Phs003508. HSC: hematopoietic stem cells; GMP: granulocyte-macrophage progenitors; Mono/Mac: monocytes/macrophages; cDC: classical dendritic cells; pDC: plasmacytoid dendritic cells.

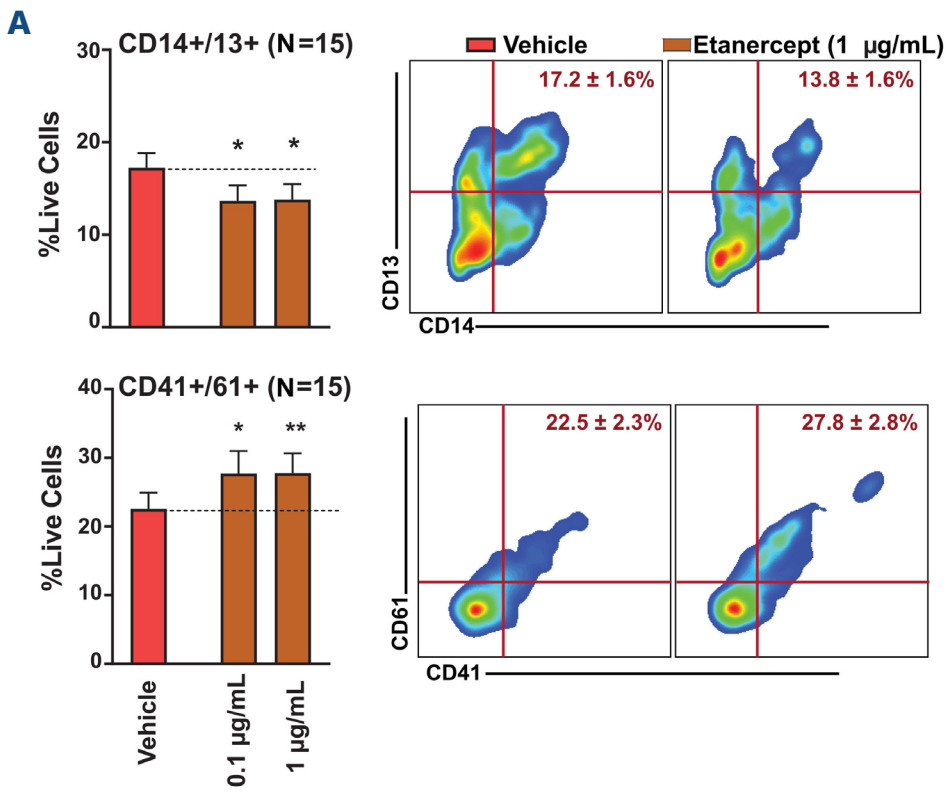

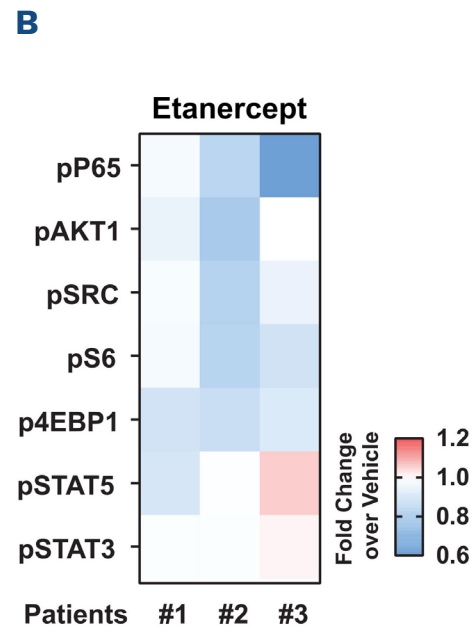

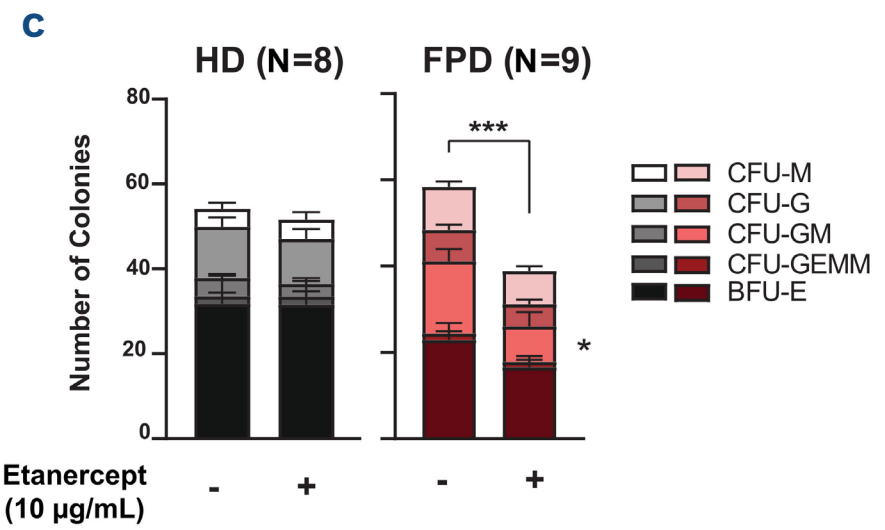

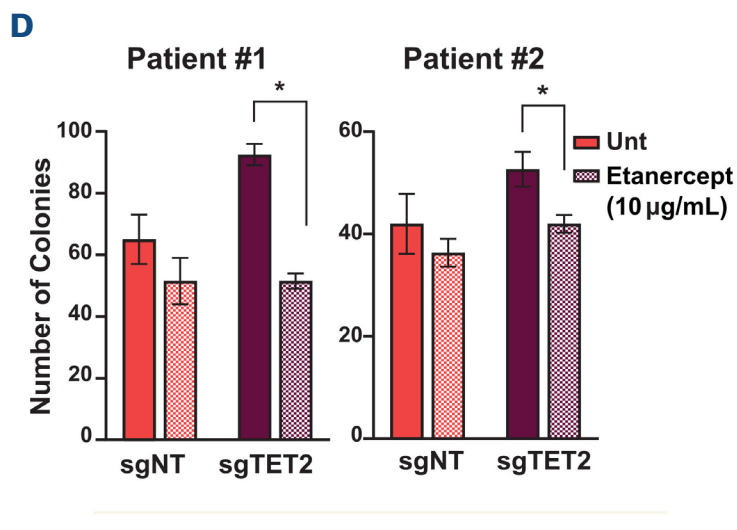

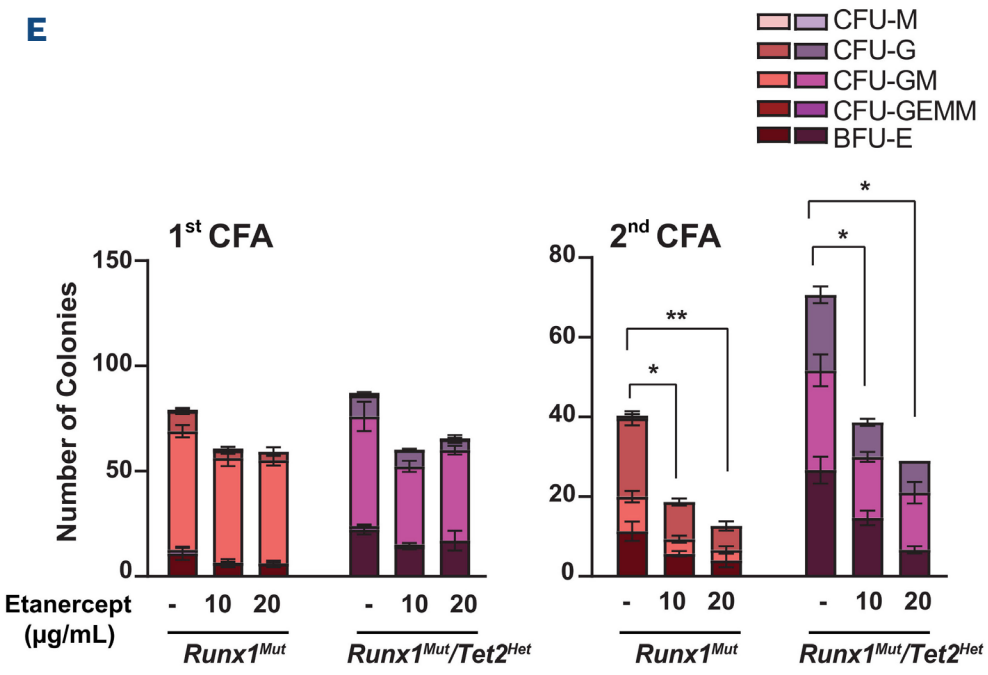

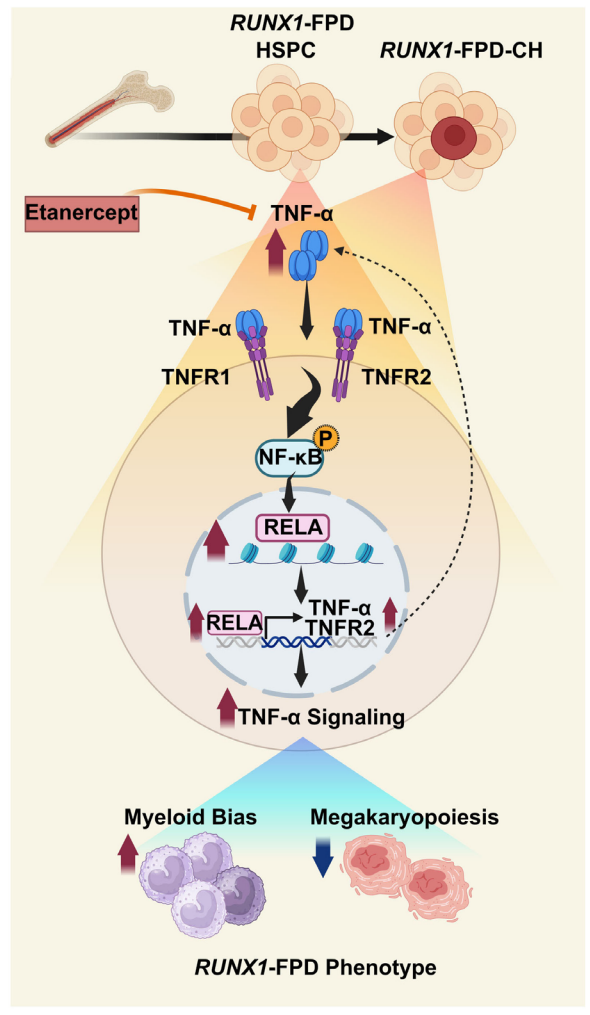

Continued on following page.

Figure 3. Tumor necrosis factor-α pathway inhibition reverses the *RUNX1*-familial platelet disorder phenotype. (A) Mononuclear cells were separated from primary *RUNX1*-familial platelet disorder (FPD, N=15) samples and used *in vitro* for culture in the presence of etanercept for 7 days. Cells were collected, and differentiation was analyzed using flow cytometry. The bar graphs show the percentages of live cells in myeloid ($CD13^+/14^+$) and megakaryocyte ($CD41^+/61^+$) populations upon treatment with etanercept at two different concentrations. A flow plot representation of the bar graphs is shown on the right. (B) *RUNX1*-FPD mononuclear cells (N=3) were cultured with etanercept (20 μg/mL) for 48 hours, and phosphorylation levels of the indicated proteins were measured through intracellular flow cytometry. (C) The results of the colony-forming assay of $CD34^+$ hematopoietic stem and progenitor cells (HSPC) from *RUNX1*-FPD patients (N=9) and healthy controls (HD, N=8) in the presence of the tumor necrosis factor (TNF)-α inhibitor, etanercept. Primary $CD34^+$ cells were seeded at a density of 1,000 cells/well (in duplicate plating) and treated with etanercept at 10 μg/mL in Methocult (StemCell, H4434). Colonies were counted on day 14 after seeding. (D) HSPC enriched from primary FPD (N=2) bone marrow samples were subject to deletion of *TET2* via the CRISPR/Cas9 method. The cells were recovered overnight in serum-free media (SEM II, StemCell) supplemented with SCF (100 ng/mL), TPO (100 ng/mL), FLT3-L (100 ng/mL), IL-6 (100 ng/mL), LDL (10 μg/mL), and UM171 (35 nM). The results of the colony-forming assay using Methocult of *TET2*-edited FPD $CD34^+$ cells (N=2, in triplicate plating) treated with etanercept and compared to non-targeted (NT)-edited cells are shown in bar graphs. (E) Heterozygous *Runx1*-knockin mice (R188Q/+, $Runx1^{Mut}$) were bred with mice harboring *Tet2*-floxed and *SCL-Cre* (JAX, 037467) alleles. The mice heterozygous for *Runx1* and *Tet2* carrying *SCL-Cre* were selected and treated with tamoxifen to activate *SCL-Cre*. Tamoxifen was dissolved in corn oil at a concentration of 30 mg/mL and mice were given a total of 100 mg/kg tamoxifen by oral gavage in 5 consecutive days. Approximately 3 weeks after the treatment, the deletion of the *Tet2*-floxed allele in peripheral blood was confirmed using polymerase chain reaction analysis. Lineage-negative cells from heterozygous *Runx1*-mutated ($Runx1^{Mut}$) and heterozygous *Runx1*-mutated with *Tet2* deletion ($Runx1^{Mut}/Tet2^{Het}$) mice were harvested. Cells were subjected to colony-forming assay using Methocult (StemCell, M3434) in the presence of etanercept at two different concentrations. The colonies were counted at 7 days after seeding and harvested for secondary plating. For primary plating, 3,000 cells/well and for secondary plating, 100,000 cells/well were used. Statistical significance was calculated using the Student *t* test and differences between untreated and treated groups are indicated as $*P \leq 0.05$, $**P \leq 0.01$, $***P \leq 0.001$. (F) Schematic showing TNF-α inhibition by etanercept reverses myeloid bias and promotes megakaryopoiesis in *RUNX1*-familial platelet disorder *in vitro* (BioRender.com/er8qn93). CFU-M: colony-forming unit (CFU)–macrophage; CFU-G: CFU–granulocyte; CFU-GM: CFU–granulocyte/monocyte; CFU-GEMM: colony-forming unit–granulocyte, erythrocyte, megakaryocyte, monocyte; BFU-E: burst-forming unit–erythroid. Unt: untreated; sgNT: single-guide non-targeting control; CFA: colony-forming assay.

Often, the transition of *RUNX1*-FPD to leukemia is accompanied by an intermediate stage of clonal hematopoiesis due to the acquisition of somatic mutations in genes such as *TET2*. An estimated 10-22% of *RUNX1*-FPD patients have *TET2* mutations.[12] *TET2* loss-of-function mutations are commonly found in clonal hematopoiesis, myelodysplastic syndromes, and AML and are associated with a poor prognosis.[13] *TET2*-mutated HSPC have been shown to have an advantage in expansion with myeloid skewing and resistance to apoptosis in the chronic presence of TNF-α.[14] Additionally, increased TNF-α levels in aged $Tet2^{-/-}$ mice led to the expansion of HSC and myeloid skewing.[15] Thus, we tested the effect of etanercept on the expansion of *TET2*-mutated cells. For this, we CRISPR-edited *TET2* in *RUNX1*-FPD HSPC and performed a colony-forming assay. *TET2* editing in *RUNX1*-FPD progenitors caused a slight increase in the colony-forming ability of *RUNX1*-FPD compared to non-targeting control (Figure 3D). Etanercept significantly reduced the colony-forming ability of *TET2*-edited *RUNX1*-FPD cells, a reduction that was more pronounced than that of non-*TET2*-edited *RUNX1*-FPD progenitors. We used murine progenitors harboring a heterozygous germline *Runx1* mutation (R188Q) and a heterozygous deletion of *Tet2* ($Runx1^{Mut}/Tet2^{Het}$). These experiments were conducted in accordance with the Oregon Health and Science University Institutional Animal Care and Use Committee guidelines. We found that etanercept significantly suppressed colony growth in both $Runx1^{Mut}$ and $Runx1^{Mut}/Tet2^{Het}$ progenitors (Figure 3E). These results demonstrate the effectiveness of etanercept in inhibiting the growth of *RUNX1*-FPD HSPC with *TET2* loss-of-function mutations. Since MIF/CD74 inhibitors are not currently accessible clinically, exploring the repurposing of etanercept to inhibit TNF-α signaling as a potential approach may increase *RUNX1*-FPD megakaryocytic differentiation while suppressing myelopoiesis.

Authors

Mona Mohammadhosseini,[1-4*] Aishwarya Sahasrabudhe,[1-4*] Luiza H. Ostrowski,[1-4] John McClatchy,[1-4] Rebekah Knight,[5] Kathryn Schabel,[6] Ryland Kagan,[6] Erica Bresciani,[7] Paul Liu[7] and Anupriya Agarwal[1-4]

[1]The Knight Cancer Institute, Oregon Health and Science University, Portland, OR; [2]Division of Oncological Sciences, Oregon Health and Science University, Portland, OR; [3]Department of Cell, Developmental, and Cancer Biology, Oregon Health & Science University, Portland, OR; [4]Department of Molecular and Medical Genetics, Oregon Health & Science University, Portland, OR; [5]Cellular Therapy Laboratory, Oregon Health and Science University, Portland, OR; [6]Department of Orthopedics & Rehabilitation, Oregon Health and Science University, Portland, OR and [7]Oncogenesis and Development Section, Division of Intramural Research, National Human Genome Research Institute, NIH, Bethesda, MD, USA

**MM and AS contributed equally as first authors.*

Correspondence:
A. AGARWAL - agarwala@ohsu.edu

https://doi.org/10.3324/haematol.2025.288410

Received: July 10, 2025.
Accepted: October 24, 2025.
Early view: November 6, 2025.

Disclosures

No conflicts of interest to disclose.

Contributions

AA provided project oversight for experimental design, data analysis, interpretation, methods development, and resources. MM designed and performed most of the experiments, analyzed the data, and was supported by AA and AS for the experiments. MM and AS performed single-cell and bulk-sequencing experiments. LHO and MM performed transcriptomic analyses. JM contributed to the development of the murine model. RKn, KS, RKa, EB and PL provided critical resources and guidance for patients' samples. All the authors wrote or edited the manuscript, provided feedback, and agreed to submit the manuscript.

Acknowledgments

We thank Oregon Health and Science University (OHSU) Massively Parallel Sequencing Shared Resource, Flow Cytometry, and Knight Biorepository, as well as the OHSU Department of Comparative Medicine, for support. We thank Hsin-Yun Lin for providing guidance in performing some experiments.

Funding

Funding for this project was provided by the Edward P. Evans Foundation and the RUNX1 Research Program AA, the Chan Zuckerberg Initiative (AA., the National Heart, Lung, and Blood Institute (R01 HL155426-01: AA); and the National Cancer Institute (U01 CA257666: AA). AA is also supported by grants from the Alex Lemonade Stand Foundation and RUNX1 Research Program, the National Cancer Institute (U01 CA229875), the National Cancer Institute (U54 CA224019) as well as Knight Cancer Research Institute pilot research projects and exploratory seed grant. MM is supported by institutional T32 (T32CA254888); Oregon Health and Science University COVID research funds; and National Heart, Lung, and Blood Institute NRSA F31 (F31HL162542). LHO is supported by ARC under award number S10OD034224. The collection of FPD samples was partly supported by intramural research programs of the National Human Genome Research Institute (EB and PL).

Data-sharing statement

The data that support the findings of this study are available as a supplementary file and can be requested from the corresponding author.

References

1. Rio-Machin A, Vulliamy T, Hug N, et al. The complex genetic landscape of familial MDS and AML reveals pathogenic germline variants. Nat Commun. 2020;11(1):1044.
2. Luo X, Feurstein S, Mohan S, et al. ClinGen Myeloid Malignancy Variant Curation Expert Panel recommendations for germline RUNX1 variants. Blood Adv. 2019;3(20):2962-2979.
3. West AH, Godley LA, Churpek JE. Familial myelodysplastic syndrome/acute leukemia syndromes: a review and utility for translational investigations. Ann N Y Acad Sci. 2014;1310(1):111-118.
4. Mohammadhosseini M, Enright T, Duvall A, et al. Targeting the CD74 signaling axis suppresses inflammation and rescues defective hematopoiesis in RUNX1-familial platelet disorder. Sci Transl Med. 2025;17(780):eadn9832.
5. Ahmad MH, Hedge M, Wong WJ, et al. Runx1-R188Q germline mutation induces inflammation and predisposition to hematologic malignancies in mice. Blood Adv. 2023;7(23):7304-7318.
6. Zezulin AU, Yen D, Ye D, et al. RUNX1 is required in granulocyte-monocyte progenitors to attenuate inflammatory cytokine production by neutrophils. Genes Dev. 2023;37(13-14):605-620.
7. Verma S, Singh A, Yadav G, et al. Serum tumor necrosis factor-alpha levels in acute leukemia and its prognostic significance. Cureus. 2022;14(5):e24835.
8. SanMiguel JM, Eudy E, Loberg MA, et al. Distinct tumor necrosis factor alpha receptors dictate stem cell fitness versus lineage output in Dnmt3a-mutant clonal hematopoiesis. Cancer Discov. 2022;12(12):2763-2773.
9. Roger T, Chanson AL, Knaup-Reymond M, Calandra T. Macrophage migration inhibitory factor promotes innate immune responses by suppressing glucocorticoid-induced expression of mitogen-activated protein kinase phosphatase-1. Eur J Immunol. 2005;35(12):3405-3413.
10. Cao L, Wang X, Liu X, et al. Tumor necrosis factor α–dependent lung inflammation promotes the progression of lung adenocarcinoma originating from alveolar type II cells by upregulating MIF-CD74. Lab Invest. 2023;103(3):100034.
11. Haraoui B, Bykerk V. Etanercept in the treatment of rheumatoid arthritis. Ther Clin Risk Manag. 2007;3(1):99-105.
12. Brown AL, Arts P, Carmichael CL, et al. RUNX1-mutated families show phenotype heterogeneity and a somatic mutation profile unique to germline predisposed AML. Blood Adv. 2020;4(6):1131-1144.
13. Chou W-C, Chou S-C, Liu C-Y, et al. TET2 mutation is an unfavorable prognostic factor in acute myeloid leukemia patients with intermediate-risk cytogenetics. Blood. 2011;118(14):3803-3810.
14. Abegunde SO, Buckstein R, Wells RA, Rauh MJ. An inflammatory environment containing TNFα favors Tet2-mutant clonal hematopoiesis. Exp Hematol. 2018;59:60-65.
15. Quin C, DeJong E, McNaughton AJM, et al. Chronic TNF in the aging microenvironment exacerbates TET2-loss-of-function myeloid expansion. Blood. 2023;142(Supplement 1):938.